Stopping and initiation of a chemical pulse at the interface of excitable media with different diffusivity

Jun Miyazaki* and Shuichi Kinoshita
Graduate School of Frontier Biosciences, Osaka University, Suita 565-0871, Osaka, Japan
(Received 30 July 2007; published 4 December 2007)

The dynamics of a chemical pulse at the interface of excitable media having different diffusion properties is presented experimentally using the Belousov-Zhabotinsky reaction system. When a chemical pulse propagates from a larger diffusion region to a smaller diffusion region, it stops and forms a steady excitation band at the interface. Furthermore, a pulse train stimulated by this band appears subsequently. A simple one-dimensional model with discontinuous diffusion is proposed, and a numerical simulation is performed that shows good agreement with the experiment. Unidirectional pulse propagation across the interface is strongly suggested on the basis of the proposed model.

DOI: 10.1103/PhysRevE.76.066201 PACS number(s): 89.75.Kd, 82.40.Ck, 82.20.−w

I. INTRODUCTION

Pulse propagation in excitable systems has attracted considerable attention in a variety of fields such as biological, chemical, and ecological systems. For example, in nerve cells, it is known that the action potential propagates along an axon with a constant velocity and amplitude [1]. This temporal change serves as the signal transmission, thereby playing a fundamental role in information processing in neuronal systems.

Although considerable effort has been devoted to the case of a spatially homogeneous medium, most of the excitable media appearing in natural systems are more or less inhomogeneous, owing to the concentration gradients, fluid flow, and embedded structures such as membranes and gels. For an inhomogeneous system, the reaction and diffusion properties vary in space, normally leading to a space dependence in the velocity of traveling pulses. In particular, it is quite interesting to clarify the mechanism of pulse propagation across the interface between different media.

Several experimental studies have been conducted on the pulse propagation in an inhomogeneous medium using the Belousov-Zhabotinsky (BZ) reaction. The BZ reaction is known to be a typical reaction-diffusion system, in which the chemical pulses propagate with a constant velocity and amplitude, exhibiting a strong similarity to the pulses in nerve cells [2,3]. Since the mechanism of the BZ reaction has been well established, it serves as a suitable model system to study various nonlinear phenomena such as free-running chemical motors [4], synchronization of coupled oscillators [5,6], and the pulse propagation in inhomogeneous media [7–9].

It has been reported that the differences in propagation velocity are realized by light illumination on a photosensitive BZ reaction [7,8] and also in the gel system by using oxygen inhibition in the reaction [9]. Refraction and reflection are observed in such systems and these observations have some analogy with those of electromagnetic and acoustic waves. In these systems, the difference in propagation velocity is due to the different reaction properties of the media, and hence the velocity difference is not so large. Consequently, the effect of the interface on the pulse propagation is not fully understand thus far, which would explicitly appear when the propagation velocity has a large difference.

In the present study, by controlling the magnitude of mass dispersion, we will develop an experimental system of the BZ reaction that has a large difference in the propagation speed. The local velocity of the chemical pulses is normally proportional to the square root of the mass diffusion coefficient. We employ a long cylindrical reactor, in which stirring is performed by a magnetically driven stirrer ball rotating at the bottom of the reactor. In such a system, the magnitude of mass dispersion has a large difference along the length of the reactor, which provides a simple one-dimensional case for the study of the propagation of the chemical pulse through the large difference in speed. We can find phenomena in this system: the stopping and generation of a pulse train at the interface where the magnitude of mass diffusion exhibits a sharp difference. We show the results of numerical simulation and put forward an analysis method to explain the experimental findings. Asymmetrical behavior of the propagation of a chemical pulse across the interface is also discussed.

II. EXPERIMENTAL PROCEDURE

Figure 1(a) shows the schematic representation of the reactor that is made of a glass cylinder with a length of 84 mm and an inner diameter of 3.7 mm. Both the ends of the cylinder were sealed with Teflon covers. Each cover had a small hole at its center, to which a Teflon tube was connected in such a way that it served as an inlet (or an outlet) to the reactor. The reactor was immersed in a water bath (24 °C) and suspended vertically. A spherical Teflon stirring ball (ϕ=3.4 mm) was placed at the bottom of the reactor, which was driven by a magnetic stirrer (EYELA: RCX1000).

The inner diameter of the cylinder and the stirring speed of the magnetic ball are essential in the present experiment. This was because the Reynolds number of this system would be defined as $\mathrm{Re}=f\pi d^2/\nu$, where f is the rotation frequency, d the diameter of the stirring ball, and ν the kinematic viscosity of water, which is a value of 1 mm^2/s. In order to

*miyazaki@fbs.osaka-u.ac.jp

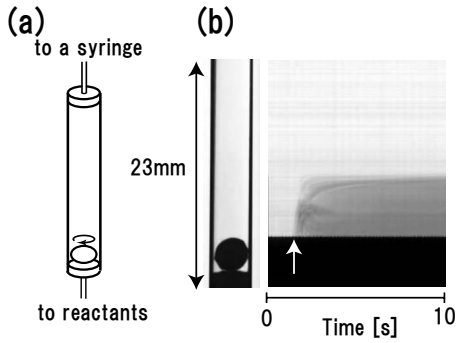

FIG. 1. (a) Schematic representation of the experimental system. (b) A photograph of the reactor and spatiotemporal plot showing the effect of stirring, which was generated by aligning the lines at the center of the reactor. The arrow shows the time at which a small amount of $Fe(phen)_3^{2+}$ solution was instantaneously injected from the bottom.

induce turbulent flow, it was necessary for Re to take a value greater than 1×10^3. We employed a stirring speed of 1000 rpm corresponding to $\sim Re=6\times10^2$. Thus the liquid in the vicinity of the stirrer ball was near the transition region from laminar to turbulent flow. However, this condition was sufficient for our purpose, as will be described later. In the regions further away, the effect of the stirring was very small and the liquid exhibited an extremely slow laminar flow or it was stagnant.

The BZ solution in the oscillatory state comprised 0.1 M $NaBrO_3$, 0.05 M malonic acid, 0.1 M H_2SO_4, and 0.86 mM $Fe(phen)_3^{2+}$. Water was prepared using a Millipore Milli-Q system. $Fe(phen)_3^{2+}$ was synthesized by mixing 1,10-phenanthroline and ferrous sulfate with the molar ratio of 3:1. All the chemicals were of analytical grade and they were used without further purification. The experiments were conducted as follows. First, the stock solutions of $NaBrO_3$, malonic acid, H_2SO_4, and $Fe(phen)_3^{2+}$ were mixed in a glass beaker. The solution was then injected through the bottom inlet into the reactor by using a syringe until the reactor was completely filled.

The spatial and temporal variations of the BZ solution were monitored by employing a CMOS camera (pixeLINK: PL-A 741). A fluorescent lamp was placed behind the reactor and used as a backlight. In order to enhance the contrast of the images, a blue optical filter was placed on the camera lens.

III. EXPERIMENTAL RESULTS

Before observing the behavior of the chemical pulses, we examined the effect of the stirring in the reactor. This is observed in such a way that the reactor is initially filled with water and then a small amount of $Fe(phen)_3^{2+}$ solution, which serves as a visible probe, is instantaneously injected from the bottom inlet. We have added NaCl into water to equalize the densities of both the solutions. Figure 1(b) shows the effect of stirring on the reactor in the form of a spatiotemporal plot. It was found that the region in the reactor is clearly separated into two parts: the lower part in the reactor is vigorously

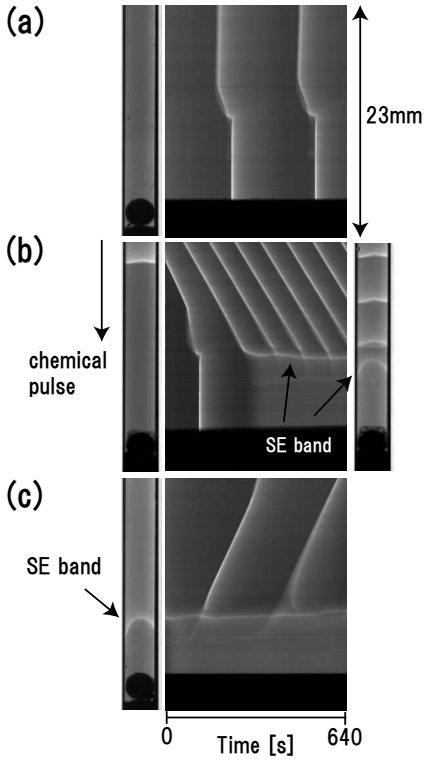

FIG. 2. Experimental results of the propagating chemical pulse in the reactor, in which the magnitude of mass diffusion exhibits a sharp difference. (a) Oscillation is observed in all the regions at the beginning of the experiment. (b) Pulse train propagates downward and then a SE band is formed at the interface between the stirred and almost unstirred regions. (c) Chemical pulses are initiated from the SE band and they propagate upward. Darker and brighter areas correspond to reduced and oxidized states of the BZ solution, respectively. Note that a slight shift of the position of the interface between the two regions seen in (b) and (c) was caused by the attachment of gas bubbles at the end covers and the stirring ball.

stirred, while the upper part remains almost unstirred. Complete mixing in the lower part occurs at a time scale of less than 1 s.

Next, we observed the dynamical behavior of the BZ reaction by filling the reactor with the reactant solution. The reactor initially exhibits the oscillation almost in unison throughout the mixed and unmixed regions, as shown in Fig. 2(a). The oscillation period is about 290 s. After several hundred seconds, traveling pulses appear in the upper part, probably initiated at a certain defect on the glass surface, as is usually the case for the BZ reaction without flow. The pulse train propagates toward the lower part with a period of 100 s and activates the lower part almost uniformly. After the first pulse (or occasionally, the first several pulses) propagates, the subsequent pulse reaches the interface where the magnitude of mass diffusion exhibits a sharp difference. However, it is found that the pulse no longer propagates and stays at the interface forming an arch-shaped steady excitation band (denoted as SE band hereafter), as shown in Fig. 2(b). In this case, although the solution in the lower part is weakly oxidized, the activation (and oscillation) in this part is completely quenched. The width of the SE band is estimated to

be less than 1 mm. Once the SE band is formed, subsequent propagating pulses collide with the SE band and disappear while the band remains. It is observed that the SE band is formed almost invariably under the present condition.

It is confirmed that the SE band is stably maintained even when the pulse train from the upper part accidentally disappears. In this case, the SE band serves as a pacemaker, from which the pulse train is initiated and it is propagated upward with a period of approximately 280 s, as shown in Fig. 2(c). It is observed that the pulse is initiated in such a way that the solution near the SE band is weakly oxidized and then it develops into a clear chemical pulse propagating upward. We have confirmed the reproducibility of these experimental results through the repeated experiments. Chemical pulses are always initiated from the SE band when no extra pulse appears, while the pulse train from the upper part is sometimes observed to disappear.

IV. THEORETICAL MODEL AND NUMERICAL SIMULATION

In the above-mentioned experiment, we observed that a chemical pulse initially passes through the interface, where the magnitudes of mass diffusion exhibit a sharp difference. After then, the subsequent pulse stops at the interface and a SE band is formed. Once the SE band is formed, the oscillation is quenched in the lower part. Furthermore, the chemical pulses propagating upward are initiated from the SE band when no extra pulse from the upper region reaches the SE band.

In order to analyze these phenomena, we will first consider the expression of the mass transfer in the present system. The simplest model of mass transport due to the random flow is usually expressed in a form analogous to the molecular diffusion as [10,11]

$$\mathbf{J} = -D_{\mathrm{eff}} \nabla C, \tag{1}$$

where D_{eff} is the effective diffusion coefficient reflecting both molecular diffusion and advection due to fluid flow. The quantity C represents concentration. The expression in Eq. (1) is valid when the time scale of mass diffusion on a macroscopic scale is shorter than the reaction time scale, which is satisfied in the present system as described subsequently.

Based on the above considerations along with the experimental observation, we introduce a reduced model for the problem; the present system can be regarded as a one-dimensional reaction-diffusion system with discontinuous diffusion coefficients, as schematically illustrated in Fig. 3(a). In this model, the dispersion due to fluid mixing is dominant in the lower region, while that due to molecular diffusion is dominant in the upper region. Hereafter, we specify the two characteristic regions as the fluid mixing region (F region) and molecular diffusion region (M region). It is assumed that the reactor is homogeneous along the transverse direction, and the concentration and its flux are both continuous at the interface.

The governing equations are then given by using the two-variable version of the Oregonator model [12,13] as

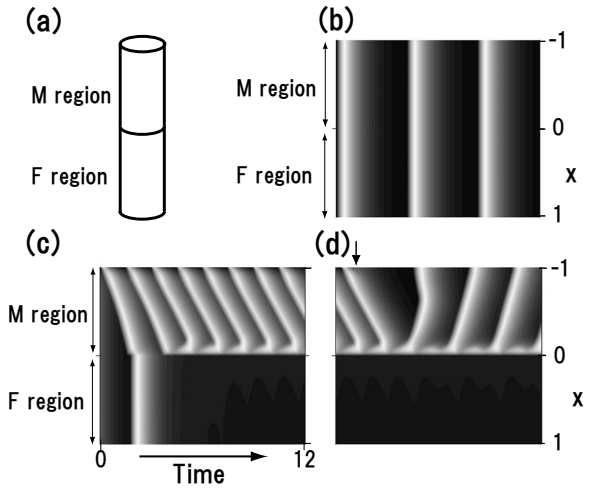

FIG. 3. (a) Schematic representation of the model having discontinuous diffusion coefficients. The upper and lower parts (M and F regions) have the diffusion coefficients, mainly due to molecular diffusion D_m and fluid flow D_f, respectively, the ratio of which is set to be $D_m/D_f=1\times10^{-3}$ in the numerical calculation. Density plots of v are shown in (b), (c), and (d) in the form of spatiotemporal plots: (b) homogeneous oscillation, (c) propagation failure of a chemical pulse accompanied by the formation of a SE band at the interface, and (d) initiation of a pulse train from the SE band when no extra pulse from the upper side reaches the interface. The arrow in (d) shows the time at which the time step at $x=-1$ is reset to its initial value so that the pacemaker disappears. After the pacemaker disappears, a phase wave appears transiently, which seemingly propagates to the M region and then collides with a pulse initiated from the SE band. After this, a stable generation of chemical pulses from the SE band is observed.

$$\frac{\partial u}{\partial t} = \epsilon^{-1}\left(u(1-u) - gv\frac{u-q}{u+q}\right) + \frac{\partial}{\partial x}\left(D(x)\frac{\partial u}{\partial x}\right),$$

$$\frac{\partial v}{\partial t} = u - v + \frac{\partial}{\partial x}\left(D(x)\frac{\partial v}{\partial x}\right), \tag{2}$$

where u and v correspond to dimensionless variables for the concentrations of $HBrO_2$ and $Fe(phen)_3^{2+}$, respectively. ϵ and q are dimensionless parameters, and g is a stoichiometric parameter. The diffusion coefficient is given as $D(x)=D_m$ for the M region, and $D(x)=D_f$ for the F region. Here, D_m denotes the molecular diffusion coefficient that is normally assumed to be of the order of 10^{-3} mm^2 s^{-1}. On the other hand, D_f is estimated from the relation $l\sim\sqrt{D_f\tau}$, where l is the characteristic distance to which molecules are transported within a time interval of τ. The length of the F region along the reactor is 10 mm, and the characteristic time scale of mass dispersion throughout this region is estimated to be ~1 s; this leads to an estimated D_f of $\sim10^2$ mm^2 s^{-1}. Note that the time scale of mass dissipation in the F region is much shorter than the characteristic time scale of oscillation, which ensures the validity of the relation in Eq. (1). The ratio of the magnitude of the diffusion coefficients is thus estimated to be $\sim10^5$. The diffusion coefficients for the variables u and v are assumed to be identical for simplicity.

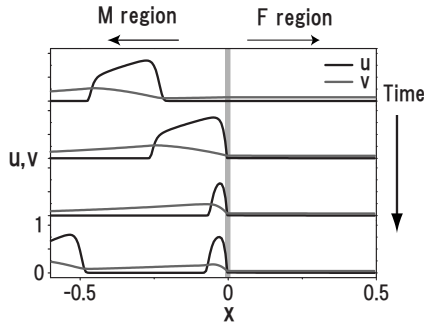

FIG. 4. Temporal evolution of u and v showing the propagation failure and the SE band formation, which corresponds to Fig. 3(c). The black and gray lines represent u and v in the Oregonator model.

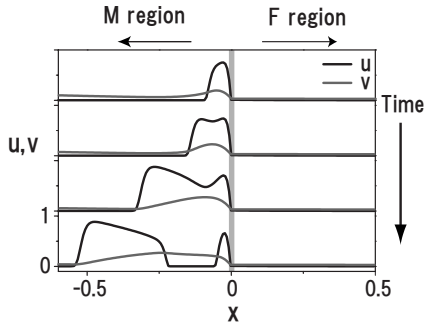

FIG. 5. Temporal evolution of u and v showing the initiation of a pulse from the SE band, which corresponds to Fig. 3(d). The black and gray lines represent u and v.

To confirm the validity of the above-mentioned model, we performed a numerical calculation using Eq. (2) for the spatiotemporal profile of the BZ reaction. The parameter values were chosen in such a way that the system is in the oscillatory regime: $q=0.002$, $g=1.0$, and $\epsilon=0.01$ with $D_m=4.5\times10^{-3}$ and $D_f=4.5$. The M and F regions are defined for the intervals $-1<x<0$ and $0<x<1$, respectively, with the Neumann boundary condition at both the end points ($x=\pm1$) to ensure zero flux. Equation (2) was calculated using a Euler method with a time step of $\Delta t=1\times10^{-6}$ and a grid size of $\Delta x=6.7\times10^{-3}$ in an array of 300 points.

The result of the numerical simulation is shown in Fig. 3. First, the system is set to be homogeneous. In this case, the diffusion term does not play any role and the oscillation occurs completely in unison over all the regions, as a trivial result of the Oregonator model [Fig. 3(b)]. The difference between the experiment and simulation is explained in terms of that a transient phase wave initially appears in the experiment owing to some heterogeneity, which propagates rapidly through the reactor followed by the almost simultaneous activation in the F region.

Next, we place a pacemaker at a point $x=-1$, at which we reset the time step to $\Delta t=2.8\times10^{-6}$ so that the natural frequency is 2.8 times as fast as that of the other points. The pacemaker initiates a series of pulses propagating toward the F region, as shown in Fig. 3(c). When the first pulse reaches the interface between the F and M regions, the F region is then activated almost uniformly. After then, it is found that the subsequent pulse stops at the interface. Figure 4 explicitly shows the temporal evolution of u and v when a pulse stops at the interface. When the pulse reaches the interface, it is found that the front part of the pulse stops at the interface. Subsequently, the back part of the pulse stops almost behind the front part, and as a result, a SE band appears. After the SE band is formed, it is found that v is accumulated around the interface and the oscillation in the F region is completely quenched. Subsequent traveling pulses annihilate after colliding with the SE band while the band remains.

The SE band is stably maintained even if a series of pulses is no longer initiated from the pacemaker. This can be examined by artificially resetting the time step at the end point to its initial value after the SE band is formed [Fig. 3(d)]. In this case, contrarily, the chemical pulses are initiated from the SE band and they propagate in the opposite directions. Figure 5 explicitly shows the temporal evolution of u and v, where a new pulse splits off from the SE band. The oscillation in the F region is still completely quenched. These results agree quite well with the experimental results.

It is interesting to study the case when the diffusion coefficient has smooth transition between the F and M regions. We have confirmed the effect of the smooth transition by linearly changing the diffusion coefficients in the transition region, while those within the F and M regions are kept constant. When the thickness of the transition region is less than about 0.2, no qualitative change is observed including the width of the SE band. With further increasing the thickness of the transition region, it is observed that the chemical pulse no longer stops and just propagates into the F region. Thus, the sharpness of the transition region will play a key role in the experiment.

V. THEORETICAL CONSIDERATIONS AND DISCUSSION

In the above-mentioned experiment and numerical simulation, we have found quite interesting results with regard to the behavior of chemical pulses at the interface. These results are summarized as follows.

(1) The first pulse (or occasionally the first several pulses) from a pacemaker propagates through the interface, and then the subsequent pulse stops at the interface leading to the formation of a SE band.

(2) Once the SE band is formed, it is stably maintained and the oscillation in the F region is completely quenched.

(3) When no extra pulse reaches the interface, a new pulse train is initiated from the SE band, which propagates in the M region.

In the following, we will provide a theoretical analysis for these peculiar phenomena concerning a chemical pulse propagation in the presence of discontinuous media on the basis of the reduced one-dimensional model presented in the foregoing section.

First, we will clarify the underlying mechanism responsible for the propagation failure at the interface by using Eq. (2). Since the value of ϵ in Eq. (2) is considerably smaller than unity, the variable u varies abruptly in space as compared with v. This abrupt change in u is often regarded as a kink. It is often assumed that in the vicinity of a kink, v is considered as a constant parameter, which leads us to de-

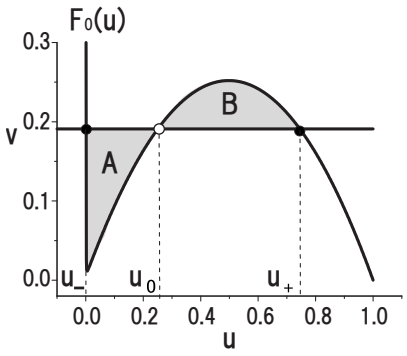

FIG. 6. A curve of $F_0(u)$ is plotted to show the static solutions of $\partial u/\partial t = F(u;v)$ with an appropriate v. Stable and unstable solutions are shown as solid and open circles, respectively. The parameter of $F_0(u)$ is $q=0.002$. The area B-A corresponds to $\Psi(v)$ in Eq. (6).

scribe the kink dynamics by the following equation:

$$\frac{\partial u}{\partial t} = F(u;v) + \frac{\partial}{\partial x}\left(D(x)\frac{\partial u}{\partial x}\right), \tag{3}$$

where $F(u;v)=\epsilon^{-1}g(u-q)/(u+q)[F_0(u)-v]$ and $F_0(u)=u(1-u)(u+q)/[g(u-q)]$. As the first step, it is convenient to analyze Eq. (3) in the absence of the diffusion term. In a typical parameter set of the Oregonator model, the differential equation $\partial u/\partial t = F(u;v)$ has two stable solutions and one unstable solution for the range $u>q$ with an appropriate v, which is indicated as the intersection points of a line of v and a curve $F_0(u)$, as shown in Fig. 6. Hereafter, we denote the values of u at the two stable points and one unstable point as $u_\pm$ and u_0, respectively. It is obvious that the system is bistable and converges to either stable point depending on the initial position.

Next, we deal with Eq. (3) including the diffusion term under the boundary condition that u approaches the value of $u_\mp$ in the limit of $x=\pm\infty$, thereby ensuring that there is a kink between $x=-\infty$ and $x=\infty$. In this case, the propagating speed of the kink c is derived as a function of v as follows [14]. When the kink propagates in a uniform medium with a diffusion coefficient D, Eq. (3) can be transformed by substituting $z=x-ct$ into

$$-c\frac{du}{dz} = F(u;v) + D\frac{d^2u}{dz^2}. \tag{4}$$

Multiplying Eq. (4) by Ddu/dz and integrating over z, we obtain the following relation:

$$-cD\int_{-\infty}^{\infty}\left(\frac{du}{dz}\right)^2 dz = -D\int_{u_-}^{u_+} F(u;v)du + \frac{1}{2}\left[\left(D\frac{du}{dz}\right)^2\right]_{z=-\infty}^{z=+\infty}. \tag{5}$$

Since there is no flux at $z=\pm\infty$, the second term on the right-hand side of Eq. (5) should be zero, and c is given as a function of v as follows:

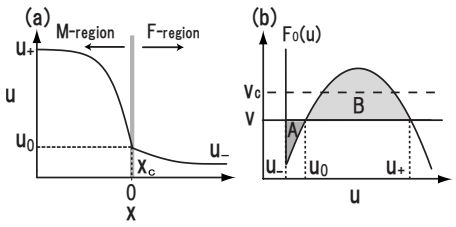

FIG. 7. (a) Schematic view of a kink at the interface, and (b) a curve of $F_0(u)$ and a line of v, which is plotted in order to show that v satisfying Eq. (9) becomes smaller than v_c when $D_m<D_f$.

$$c(v) = \frac{\Psi(v)}{D\int_{-\infty}^{\infty}(du/dz)^2 dz}, \tag{6}$$

where $\Psi(v)$ is defined as

$$\Psi(v) \equiv D\int_{u_-}^{u_+} F(u;v)du. \tag{7}$$

Because the parameter q in the Oregonator model is normally smaller than u for the integral range in Eq. (7), $(u-q)/(u+q)$ in $F(u;v)$ is roughly assumed to be unity. This allows us to replace $\Psi(v)$ by

$$\Psi(v) \sim D\epsilon^{-1}g\int_{u_-}^{u_+}[F_0(u)-v]du. \tag{8}$$

The integral part of this equation corresponds to the area B subtracted by A, as shown in Fig. 6. It is shown that $c(v)$ becomes zero when v takes a specific value of v_c such that the two areas A and B are equal. It should be noted that the kink propagates in the positive direction for $v<v_c$, while it propagates in the opposite direction for $v>v_c$.

Further, we consider the case of an inhomogeneous diffusion medium under the same boundary condition as that in the homogeneous medium. The static solution of Eq. (3) must satisfy the following relation, which is obtained by multiplying Eq. (3) by $D(x)\partial u/\partial x$ and integrating over x as

$$\bar{\Psi}(v,x_c) \equiv \epsilon^{-1}g\int_{u_-}^{u_+} D[x(u)][F_0(u)-v]du = 0. \tag{9}$$

Here, we define the center of the kink at $u=u_0$ and express the static solution of Eq. (3) as $u(x;x_c)$ in order to explicitly indicate that u is a function of x with the center of the kink placed at x_c. Note that the curve $\bar{\Psi}(v,x_c)=0$ in the vx_c plane is the zero-speed condition for a set of v and x_c, and $\bar{\Psi}(v,x_c)$ is equivalent to Eq. (8) in a homogeneous medium.

It is natural to expect that the shape and speed of a propagating kink are modulated as it approaches the interface of the two media. In order to investigate the behavior of the kink near the interface, it is useful to consider a typical case in which the center of the kink is placed at the interface, i.e., $x_c=0$, as illustrated in Fig. 7(a). Here, we assume that the interface is located at the origin and the diffusion coefficient is given as

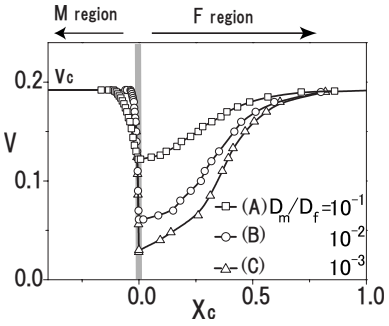

FIG. 8. Curves of $\bar{\Psi}(v,x_c)=0$ in the vx_c plane for several sets of diffusion coefficients. D_f is kept constant for (A), (B), and (C), while D_m is varied such that the ratio D_m/D_f becomes 10^{-1}, 10^{-2}, and 10^{-3}, respectively.

$$D(x) = \begin{cases} D_m, & x < 0, \\ D_f, & x > 0. \end{cases}$$

where $D_m < D_f$ and we denote the regions for $x<0$ and $x>0$ as M and F regions, respectively, in relation to the preceding section. In this case, the condition in Eq. (9) is satisfied when the area A multiplied by D_f is equal to the area B multiplied by D_m. Under the condition $D_m<D_f$, it is apparent that a smaller value of v satisfies Eq. (9) in comparison to that in a homogeneous medium, v_c, as shown in Fig. 7(b). This suggests that the curve $\bar{\Psi}(v,x_c)=0$ in the vx_c plane should have a dip at the interface. To confirm this, we have plotted the curve $\bar{\Psi}(v,x_c)=0$ by numerically calculating the static solution of Eq. (3) and evaluating x_c with varying v, as shown in Fig. 8 [15]. Several sets of diffusion coefficients are employed for the sake of comparison. A dip clearly appears at the interface, whose extremal value v_{ex} decreases with the ratio D_m/D_f.

On the basis of this, we will qualitatively explain the kink dynamics at the interface. Let us assume that v has a value of v_* at the interface such that $v_*<v_c$. When the difference between the diffusion coefficients of the two media is sufficiently large such that $v_{ex}<v_*<v_c$, the curve $\bar{\Psi}(v,x_c)=0$ has a pair of intersection points with $v=v_*$ at $x=x_\pm$, as illustrated in Fig. 9. It is shown that $\bar{\Psi}(v_*,x_c)$ is positive in the regions $x<x_-$ and $x_+<x$; this indicates that a kink in this region propagates in the positive direction of the x axis, which is consistent with the case for a homogeneous medium. On the other hand, $\bar{\Psi}(v_*,x_c)$ is negative in the region between x_- and x_+, implying that a kink propagates in the opposite direction. In this context, the points at x_- and x_+ can be regarded as an attracting point and separating point, respectively. These facts suggest that a kink propagating from the M region to the F region should stop with its center at $x=x_-$.

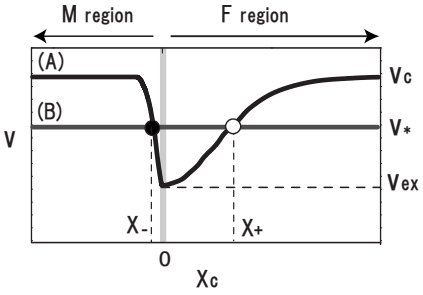

FIG. 9. Schematic representation of a curve (A) $\bar{\Psi}(v,x_c)=0$ and a line (B) $v=v_*$ around the interface. Attracting and separating points are shown as filled and open circles, respectively.

In the numerical simulation as well as in the experiment, it is observed that the first pulse (or occasionally, the first several pulses) passes through the interface and then the subsequent pulses stop. This can be explained by considering the behavior of the front kink of a traveling pulse along with the temporal variation of v_* on the basis of the above-mentioned analysis. Figure 10 shows the time course of chemical pulses at the interface and their intuitive explanations. Part (I) of Fig. 10 shows that the first pulse can propagate across the interface, because v_* is initially smaller than v_{ex}. After the propagation of the first pulse, v is transiently accumulated at the interface. When the subsequent pulse approaches successively, it is possible that v_* is larger than v_{ex}. For such v_*, Eq. (9) is satisfied, resulting in the propagation failure of the subsequent pulse [part (II) in Fig. 10].

In the above-mentioned discussion, we investigated the behavior of a pulse propagating in the media from the lower

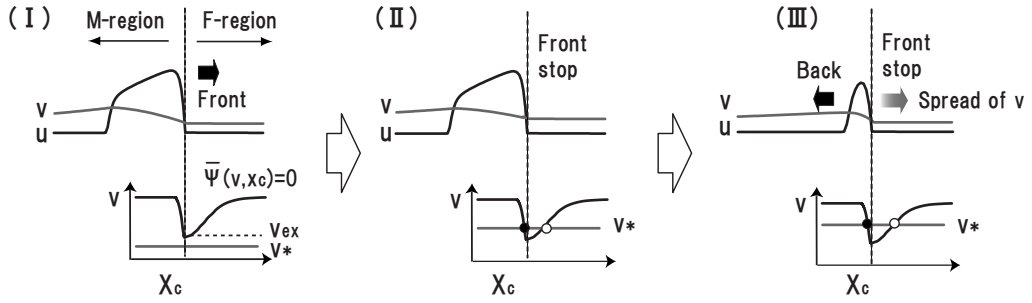

FIG. 10. Schematic illustration of the time course of traveling chemical pulses at the interface. In each figure, the upper part shows u and v in the Oregonator as a black and gray line, respectively. The lower part shows the curve $\bar{\Psi}(v,x_c)=0$ (black line) and v_* (gray line) in the vicinity of the interface. Part (I) The first pulse passes across the interface; the front kink propagates across the interface since $v_*<v_{ex}$. Part (II) After the propagation of the first pulse, the front kink of subsequent pulse stops at the interface since $v_*>v_{ex}$. Part (III) After the propagation failure, the SE band is stably maintained at the interface because v dissipates into the F region. The back kink tends to propagate in the left direction due to the repulsive interaction between the two kinks.

to the higher diffusion regions. In addition to this, it is interesting to examine the opposite case: pulse propagation from the higher to the lower diffusion regions. In order to elucidate this point, we have performed numerical simulation by using Eq. (2) for $D_m > D_f$ and confirmed that pulses simply pass through the interface. This is explained according to the above-mentioned analysis as follows: because the curve $\bar{\Psi}(v, x_c)=0$ should have a positive hump for $D_m > D_f$, Eq. (9) cannot be satisfied for small v and the pulse just passes across the interface. Thus, unidirectional pulse propagation is strongly suggested.

Unidirectional propagation of a chemical pulse is interesting because it is closely related to the signal processing in excitable systems [16–18], which has been realized experimentally in several systems such as geometrically asymmetrical two-dimensional media using photosensitive BZ reactions [16] and in membrane systems through microgaps with asymmetrical excitability [17]. Although these systems are different from that in the present study, similar analysis may be applied to explain the mechanism responsible for the unidirectional propagation. Further studies are required to clarify this point.

A few issues should be discussed to further understand the experimental results. It is found in the numerical simulation that after the front kink stops, the back kink almost stops as it approaches the front kink. The back kink then tends to propagate in the opposite direction when no extra pulse propagates from the M region. These facts may be explained by the repulsive interaction between the front and the back kinks through the slow reaction of v [19]. The front kink does not move even under the influence of repulsive interaction owing to the presence of the interface. On the other hand, the back kink propagates in the opposite direction, and accordingly results in the generation of a new pulse.

Finally, we explain that the SE band is stably maintained and the oscillation is quenched in the F region, by considering that u and v serve as an activator and an inhibitor, respectively, in the Oregonator model. After the SE band appears, the inhibitor is gradually accumulated at the interface following the high concentration of the activator, and then, the inhibitor will also spread over the F region as shown in part (III) of Fig. 10. As a result, the activation is suppressed in the F region owing to the incoming inhibitor because the inhibitor varies slowly with time, which mainly governs the reaction dynamics of the system. On the other hand, the SE band is maintained stably owing to the dispersion of the inhibitor, although it requires further analysis to clarify that the SE band is still maintained even after a new pulse splits off from the band.

In summary, we have studied the behavior of a chemical pulse encountering the interface between the media, where the magnitude of mass diffusion exhibits a sharp difference. Phenomena have been observed such as the propagation failure at the interface, SE band formation, quenching of oscillation, and initiation of a pulse from the SE band. These experimental results are well reproduced by the numerical simulation on the basis of simple one-dimensional models having discontinuous diffusion coefficients. Furthermore, we have qualitatively shown the underlying mechanism of these phenomena and have suggested the unidirectional propagation of a chemical pulse.

The results in the present study may be applied to the pattern formation in various media such as gels [20], membranes [21], ion-exchange resins [22], and microemulsions [23], where the molecular diffusivity is largely dependent on the structural properties of the medium. In addition, it is also probable in certain situations that the system is not stagnant and that the medium flows with enhanced mass transport, thereby having a significant influence on the pattern formation process [24,25]. Such chemical systems undergoing mixing are particularly interesting in that they can often be seen in nature, e.g., plankton population dynamics in ocean currents [26], reactive pollutants in atmosphere [27], and the ozone reaction in the stratosphere [28]. Thus, we believe that the present study may provide a general insight and a better understanding of these reaction-diffusion systems in a variety of fields.

ACKNOWLEDGMENTS

This work was partially supported by the Japan Society for Promotion of Science for Young Scientists.

[1] J. G. Nicholls, A. R. Martin, B. G. Wallace, and P. A. Fuchs, *From Neuron to Brain*, 4th ed. (Sinauer Associates, Sunderland, MA, 2001).
[2] A. N. Zaikin and A. M. Zhabotinsky, Nature (London) **225**, 535 (1970).
[3] I. R. Epstein and J. A. Pojman, *An Introduction to Nonlinear Chemical Dynamics: Oscillations, Waves, Patterns, and Chaos* (Oxford University Press, New York, 1998).
[4] R. Yoshida, T. Takahashi, T. Yamaguchi, and H. Ichijo, J. Am. Chem. Soc. **118**, 5134 (1996).
[5] J. Miyazaki and S. Kinoshita, Phys. Rev. Lett. **96**, 194101 (2006); Phys. Rev. E **74**, 056209 (2006).
[6] H. Fukuda, H. Morimura, and S. Kai, Physica D **205**, 80 (2005).
[7] O. Steinbock, V. S. Zykov, and S. C. Müller, Phys. Rev. E **48**, 3295 (1993).
[8] N. Manz, V. A. Davydov, V. S. Zykov, and S. C. Müller, Phys. Rev. E **66**, 036207 (2002).
[9] A. M. Zhabotinsky, M. D. Eager, and I. R. Epstein, Phys. Rev. Lett. **71**, 1526 (1993).
[10] E. L. Cussler, *Diffusion: Mass Transfer in Fluid Systems* (Cambridge University Press, Cambridge, 1984).
[11] C. Gutfinger, *Topics in Transport Phenomena: Bioprocesses, Mathematical Treatment, Mechanisms* (Hemisphere, Washington, 1975).
[12] R. J. Field and R. M. Noyes, J. Chem. Phys. **60**, 1877 (1974).

[13] J. J. Tyson and P. C. Fife, J. Chem. Phys. **73**, 2224 (1980).
[14] E. Meron, Phys. Rep. **218**, 1 (1992).
[15] The solution is estimated in such a way that the initial condition is given arbitrarily and repeatedly until a plausible solution is found by minimizing the time evolution of u in all the regions, which is confirmed to satisfy the condition $\int_{-1}^{1}(du/dt)^2dx < 1 \times 10^{-8}$.
[16] K. Agladze, R. R. Aliev, T. Yamaguchi, and K. Yoshikawa, J. Phys. Chem. **100**, 13895 (1996).
[17] K. Suzuki, T. Yoshinobu, and H. Iwasaki, J. Phys. Chem. A **104**, 6602 (2000).
[18] I. Motoike and K. Yoshikawa, Phys. Rev. E **59**, 5354 (1999).
[19] T. Ohta and J. Kiyose, J. Phys. Soc. Jpn. **65**, 1967 (1996).
[20] T. Yamaguchi, L. Kuhnert, Zs. Nagy-Ungvarai, S. C. Muller, and B. Hess, J. Phys. Chem. **95**, 5831 (1991).
[21] D. Winston, M. Arora, J. Maselko, V. Gaspar, and K. Showalter, Nature (London) **351**, 132 (1991).
[22] J. Maselko and K. Showalter, Nature (London) **339**, 609 (1989).
[23] V. K. Vanag and I. R. Epstein, Phys. Rev. Lett. **87**, 228301 (2001).
[24] C. R. Nugent, W. M. Quarles, and T. H. Solomon, Phys. Rev. Lett. **93**, 218301 (2004).
[25] Z. Neufeld, Phys. Rev. Lett. **87**, 108301 (2001).
[26] E. Abraham *et al.*, Nature (London) **407**, 727 (2000).
[27] A. Wonhas and J. C. Vassilicos, Phys. Rev. E **65**, 051111 (2002).
[28] S. Edouard, B. Legras, F. Lefevre, and R. Eymard, Nature (London) **384**, 444 (1996).